ACS APPLIED MATERIALS & INTERFACES

Research Article

www.acsami.org

# Zwitterionic Phenyl Layers: Finally, Stable, Anti-Biofouling Coatings that Do Not Passivate Electrodes

Alicia L. Gui,[†] Erwann Luais,[‡] Joshua R. Peterson, and J. Justin Gooding*

School of Chemistry and Australian Centre for NanoMedicine, The University of New South Wales, Sydney, NSW 2052, Australia

Supporting Information

**ABSTRACT:** Organic coatings on electrodes that limit biofouling by proteins but are of sufficiently low impedance to still allow Faradaic electrochemistry to proceed at the underlying electrode are described for the first time. These organic coatings formed using simple aryl diazonium salts present a zwitterionic surface and exhibit good electrochemical stability. The layers represent a low impedance alternative to the oligo (ethylene glycol) (OEG)-based anti-biofouling coatings and are expected to find applications in electrochemical biosensors and implantable electrodes. Two different zwitterionic layers grafted to glassy carbon surfaces are presented and compared to a number of better-known surfaces, including OEG-based phenyl-layer-grafted glassy carbon surfaces and OEG alkanethiol SAMs coated on gold, to allow the performance of these new layers to be compared to the body of work on other anti-biofouling surfaces. The results suggest that phenyl-based zwitterionic coatings are as effective as the OEG SAMs at resisting the nonspecific adsorption of bovine serum albumin and cytochrome c, as representative anionic and cationic proteins at physiological pH, whereas the impedance of the zwitterionic phenyl layers are two orders of magnitude lower than OEG SAMs.

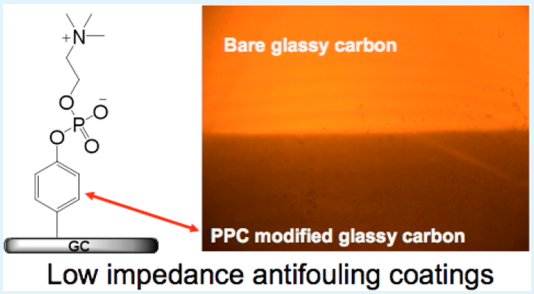


**KEYWORDS:** *aryl diazonium salts, anti-biofouling coating, low impedance, zwitterionic surfaces, fluorescence microscope imaging, phosphorylcholine*

## INTRODUCTION

There is a myriad of applications where electrodes are used in biological matrices, not least of which are electrochemical biosensors and implantable electrodes. However, placing electrodes in biological media inevitably results in nonspecific adsorption of proteins (biofouling).[1−4] In biosensors, biofouling can hinder or completely prevent analyte reaching the sensing interface and hence compromise the performance of such devices.[5−7] In vivo, for medical implants (including implantable biosensors), the biofouling often triggers "foreign body response", leading to the encapsulation of the implants into collagen plaques.[1] This biological encapsulation prevents intimate contact between the device and tissue.[1−3,8,9] For stimulating electrodes, the presence of a protein layer means higher potentials need to be applied to the electrode, which can decrease implant lifetime.[8,9] Hence, there is a clear need for anti-biofouling coatings for biosensors and medical implants.[3,4,10]

The surface chemistry that has to date been the most widespread and effective for limiting biofouling has been polyethylene glycol (PEG)[11−16] and self-assembled monolayers presenting oligo(ethylene glycol) chains (OEG-SAMs).[10,17−23] However, these anti-biofouling layers form a passivating (high impedance) layer on electrodes, in essence rendering the electrodes useless.[23] The challenge is to develop a surface chemistry for reducing biofouling on a surface that is not high impedance, such that an underlying electrode is not passivated.

We have previously demonstrated one solution to making electrodes antifouling is using OEG layers on electrodes but fabricating conducting channels through the passivating OEG layer using either molecular wires[24] or nanoparticles.[25] We have shown that electrochemical immunosensors prepared using these strategies can be used to detect analytes in whole blood.[26] However, these interfaces are complicated to fabricate, and in the case of the molecular wires, difficult to synthesize and relatively unstable. Furthermore, it is not really viable for implantable electrodes where the PEG or OEG moieties are prone to auto-oxidation in most biochemically relevant solutions.[14,27,28] Here we use a completely new strategy by forming low impedance anti-biofouling layers presenting zwitterionic properties which employ different aryl diazonium salts bearing charged functionalities and are shown to be as effective, if not more effective, than alkanethiol OEG layers on gold.

Inspiration for using zwitterions in anti-biofouling coatings can trace back to the studies by Hayward and Chapman on improving haemocompatibility of biomaterials using polymerizable phosphatidylcholines .[29] Over the last decade, PC (phosphorylcholine)-based polymers have been used in various applications which require resistance to protein adsorption, particularly implants.[26,30,31] The pioneering work of incorporat-

Received: February 7, 2013
Accepted: May 3, 2013
Published: May 3, 2013

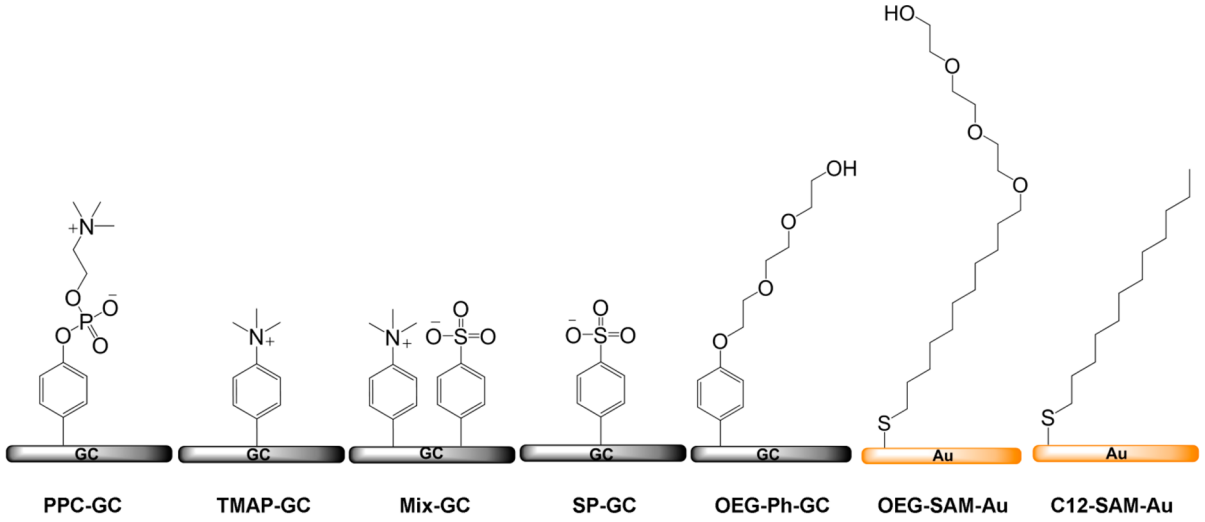


**Figure 1.** Schematic representation of glassy carbon surfaces coated with phenyl phosphorylcholine (PPC), 4-(trimethylammonio)-phenyl (TMAP), 1:1 mixed layers of 4-sulfophenyl and 4-(trimethylammonio)-phenyl (mix), 4-sulfophenyl (SP), 2-(2-(2-phenoxy)ethoxy)ethoxy)ethanol (OEG-Ph), and gold surfaces modified with SAMs of triethylene glycol mono-11-mercaptoundecyl ether (OEG-SAM) and 1-dodecanethiol (C12-SAM).

ing zwitterionic moieties into alkanethiol SAMs has been performed by Whitesides and co-workers[32] and Cooper and co-workers.[33] Holmlin et al. has found zwitterionic SAMs formed from 1:1 mixture of two long chain alkanethiols respectively bearing $-SO_3^-$ and $-N^+(Me)_3$ terminal groups performed exceptionally well at resisting protein adsorptions (comparable with OEG SAMs).[32] Single-component SAMs formed from alkanethiols with zwitterionic terminal groups $-N^+(Me)_2(CH_2)_2SO_3^-$ (sulfobetaine) and $-OP(O^-)(O)O-(CH_2)_2N^+(Me)_3$ (phosphorylcholine) are also observed to be protein resistant, but not as effective as the mixed SAMs. Jiang and co-workers have conducted an investigation into the anti-biofouling mechanism of these zwitterionic SAMs at the molecular level.[34,35] The results of their work have suggested complete charge balancing and packing of the charged groups are important to the protein resistance of the zwitterionic SAMs. In recent years, zwitterionic functionalities have been increasingly explored as layers to limit nonspecific protein adsorption.[32−39] However, again the surface chemistries employed to anchor these zwitterionic functionalities have involved long-chain aliphatic hydrocarbons, which again form a high impedance layer on an electrode.

Part of the reason long-chain alkanethiols have, for example, been used to anchor zwitterions to surfaces as anti-biofouling layers is because of the poor stability of short-chain alkanethiols.[40] We have shown recently that aryl diazonium salt derived layers can form far more stable layers, with similar sensing performance, for electrochemical sensing on gold electrodes.[41] Details of aryl diazonium salt surface modification ranging from the reaction mechanism to different applications can be easily accessed in literatures.[40−43]

The purpose of this paper is to show the utility of combining zwitterionic surfaces with aryl diazonium salts to create low impedance anti-biofouling layers on electrodes. We present two novel zwitterionic phenyl layers, one bearing a 1:1 mixture of single charged ($-SO_3^-$ and $-N^+(Me)_3$) moieties to form a zwitterionic surface and another where the zwitterion phenyl phosphorylcholine is attached to a glassy carbon electrode. The ability of these layers to limit nonspecific adsorption of protein are compared with more conventional OEG phenyl layers formed from deposition of OEG aryl diazonium salt and the "standard" of anti-biofouling systems OEG alkanethiol SAMs on gold. Figure 1 shows schematic illustrations of the seven different electrode surface chemistries studied in this paper. The designations PPC-GC, TMAP-GC, mix-GC, SP-GC, OEG-Ph-GC, OEG-SAM-Au, and C12-SAM-Au are used to refer to these coated electrode surfaces throughout the paper. The evaluation of protein adsorption on these surfaces was carried out using fluorescence microscope imaging, which has been widely used for visualization[44−46] and relative quantification[45,47−49] of protein adsorption on a wide range of materials.[50−55] The microscopic images were used to examine the spatial distribution and the status (such as aggregation) of the proteins adsorbed on the surfaces together with a quantitative comparison of the protein adsorption level on different surfaces. Subsequently the impedance of the layers was evaluated by measuring the charge transfer resistance ($R_{ct}$) using electrochemical impedance spectroscopy (EIS). The electrochemical stability of these layers has also been investigated in the current study as it is relevant to future applications.

## EXPERIMENTAL METHODS

**Reagents and Materials.** Tetrabutylammonium tetrafluoroborate ($NBu_4BF_4$), sodium nitrite ($NaNO_2$), potassium chloride (KCl), potassium dihydrogen phosphate ($KH_2PO_4$), potassium phosphate dibasic ($K_2HPO_4$), fluoroboric acid ($HBF_4$, 48%), potassium ferricyanide ($K_3Fe(CN)_6$), hexammine ruthenium(III) chloride ($Ru(NH_3)_6Cl_3$), sodium carbonate ($Na_2CO_3$), sodium bicarbonate ($NaHCO_3$), rhodamine B isothiocyanate ($C_{29}H_{30}ClN_3O_3S$), triethylene glycol mono-11-mercaptoundecyl ether ($C_{17}H_{36}O_4S$), 1-dodecanethiol ($C_{12}H_{25}SH$), and acetonitrile ($CH_3CN$, HPLC grade) were obtained from Sigma-Aldrich (Sydney, Australia). 4-Aminophenyl phosphorylcholine ($C_{11}H_{19}N_2O_4P$) was purchased from TRC (Canada). Acetic acid ($CH_3COOH$), hydrogen peroxide ($H_2O_2$), dimethyl sulphoxide ($(CH_3)_2SO$), hydrochloric acid (HCl, 32%), sulfuric acid ($H_2SO_4$, 98%), and glycerol ($C_3H_8O_3$) were obtained from Ajax Finechem (Sydney, Australia). All reagents were used as received, and aqueous solutions were prepared with Milli-Q water (18 MW $cm^{-1}$, Millipore, Sydney, Australia).

**Proteins.** Bovine serum albumin-fluorescein isothiocyanate (BSA-FITC) and cytochrome *c* (from bovine heart) were obtained from Sigma (Sydney, Australia). The cytochrome c (Cyt c) was then conjugated with fluorescent dye rhodamine B by following the

procedure described in Damodaran et al.[50] and Veiseh et al.[55] Ten milligrams (0.81 μmol) of cytochrome c (Cyt c) was dissolved in 1 mL of 0.1 M sodium carbonate/bicarbonate buffer (pH 9.05), and 0.25 mL (4.65 μmol) of 10 mg/mL rhodamine B isothiocyanate (RBITC) in DMSO was added, to obtain around 5-fold molar excess of RBITC to Cyt *c*. The mixture was incubated for 1 h at room temperature in the dark with continuous magnetic stirring. Separation of the RBITC-Cyt *c* conjugate from the un-reacted label was performed by two steps of filtration. First, the mixture was filtered to remove the RBITC dye precipitate through a syringe filter (0.22 μm Non-sterile 13 mm Millex, EMD Millipore USA). Then the soluble un-reacted dye was removed using an Amicon Ultra-15 centrifugal filter device (3 kDa MW cutoff, EMD Millipore USA). The purified RBITC-Cty *c* PBS solution was characterized by UV-Vis and fluorescence spectroscopy and stored in the freezer.

**Electrode Surface Pretreatment.** Glassy carbon (GC) electrodes (CH Instrument USA, 3.0 mm diameter disks) and Polycrystalline gold electrodes (CH Instruments, USA, 2.0 mm diameter disks) were cleaned by first polishing in the 1.0, 0.3, and 0.05 micrometer micropolisher (alumina slurry). GC electrodes were briefly sonicated in Milli-Q for 1−2 minutes. The cleaning of GC plates used for XPS and protein adsorption test were conducted in the same manner as for disk electrodes. The polishing of gold electrodes, however, was followed by electrochemical cleaning in 0.05 M $H_2SO_4$ by cycling the electrodes between −0.3 and 1.5 V (versus Ag/AgCl) until a reproducible voltammogram was obtained. Cleaning of gold foil used for protein adsorption study was performed by overnight immersion in piranha solution (a 1:3 mixture of 30% aqueous $H_2O_2$ solution and concentrated sulfuric acid), followed by rinsing with copious amounts of Milli-Q water.

**Glassy Carbon (GC) Surface Modification.** Surface modification of GC electrodes with phenyl derivatives bearing phosphorylcholine group (PPC) and phenyl derivatives bearing hydroxyl terminated oligo(ethylene glycol) functionality (OEG-Ph) was conducted by the in situ method as described in Baranton et al.[56] A 0.1 M aqueous $HBF_4$ solution containing the corresponding aniline derivative, 5 mM of 4-aminophenyl-phosphorylcholine (or 5 mM of 2-(2-(2-(4-amino-phenoxy)-ethoxy) ethoxy)ethanol) was added with equivalent amount of $NaNO_2$ as diazotization reagent. 2-(2-(2-(4-aminophenoxy)-ethoxy)ethoxy)-ethanol) was custom synthesized, the synthesis procedure has followed the published method in Liu et al.[24] The solution was purged with argon for 30 min prior to reductive adsorption, and was kept under a blanket of argon during surface modification. The reductive adsorption of in situ generated PPC diazonium salt and OEG-Ph diazonium salt were performed by 3 cycles of cyclic voltammetry scans from 0.7 V to −1 V, at 100 mV/s. Glassy carbon surfaces grafted with 4-sulfophenyl (SP), 4-(trimethyl-ammonio)-phenyl (TMAP) and 1:1 SP/TMAP (mix) for comparative studies were prepared by procedure described in Gui et al.[57] Modification of glassy carbon plates for XPS characterization and protein adsorption test was performed in the same manner as that with electrodes. The glassy carbon plates were modified by dipping half of the plate into the aryl diazonium salt solution, such that the same surface could be used to observe the difference in protein adsorption on the bare glassy carbon region relative to the functionalized region.

**Gold Surface Modification with Alkanethiol SAMs.** To form alkanethiol SAMs presenting oligo(ethylene glycol) (OEG-SAM) and aliphatic hydrocarbons (C12-SAM), the cleaned gold electrode and gold foil were first soaked in distilled ethanol (99%) for 15 min to remove the surface oxide. Then the gold electrodes and gold foils were transferred into 1 mM ethanolic solutions respectively containing triethylene glycol mono-11-mercaptoundecyl ether and 1-dodecane-thiol for monolayer self-assembling over 12 h. SAMs modified gold electrodes and gold foils were thoroughly rinsed with distilled ethanol and Milli Q water before electrochemical measurements and protein adsorption experiment.

**Electrochemical Measurement.** All voltammetry measurements were performed with a μAutoLabIII potentiostat (Metrohm AutoLab B.V. Netherlands ) and a conventional three-electrode system, comprised of a GC working electrode, a platinum wire as the auxiliary electrode, and a Ag/AgCl 3.0 M NaCl electrode (CH Instrument, USA) as reference. All potentials were reported versus the Ag/AgCl reference electrode at room temperature. Data collecting and processing was performed with the operation software GPES 4.9. The electrochemical impedance spectroscopy (EIS) data were acquired using a Solartron SI 1287 electrochemical interface coupled with an SI 1260 frequency response analyser (Solartron Analytical, Hampshire, England). The measurements were performed in two aqueous solutions containing different redox probes, $Fe(CN)_6^{3-}$ and $Ru(NH_3)_6^{3+}$. The two solutions respectively contains 1 mM of one redox probe, with both containing 0.1 M of KCl for each solution as the supporting electrolyte were prepared. The EIS spectra were run over a frequency range of 0.1−100000 Hz at 0.2 V for $Fe(CN)_6^{3-}$ and an applied DC potential at −0.165 V for $Ru(NH_3)_6^{3+}$, with an amplitude of 10 mV. The Nyquist plots presenting comparison of different surfaces are provided in the Supporting Information (Figure SI 8). The spectroscopy data were analysed in ZView 3.1 and ZPlot software (Scribner Associates, Inc.). Charge transfer resistance ($R_{ct}$) was determined in ZView 3.1 by curve fitting to a conventional Randles equivalent circuit as shown below, with two variations of the Warburg element (GFW- Short Circuit Terminus for OEG-Ph-GC, OEG-SAM-Au, and C12-SAM-Au; GFW-Open Circuit Terminus for bare surfaces, PPC-GC and mix-GC).

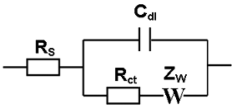


The electron transfer rate ($k_{et}$) was calculated using the Butler−Volmer equation with the obtained $R_{ct}$.

$$i_0 = FAk^0 C_O^{*(1-\alpha)} C_R^{*\alpha} \quad (1)$$

$$R_{ct} = RT/nFi_0 \quad (2)$$

In the above equations, the $i_0$ is the exchange current density (A/cm$^2$), $F$ the Faraday constant (≈96500 C/mol), $A$ the electrode active surface area (cm$^2$), $k^0$ the standard heterogeneous rate constant (cm/s), $C_O$* and $C_R$*, respectively, the bulk concentration of oxidized and reduced form of the electro active species (mol/cm$^3$), $\alpha$ the transfer coefficient (dimensionless parameter with values between 0 and 1, often estimated to be 0.5), $R$ the universal gas constant (≈ 8.31 J K$^{-1}$ mol$^{-1}$), $T$ the absolute temperature (K) and $n$ the number of electrons transferred in the electrochemical reaction.

**Fluorescence Microscope Imaging of Protein Adsorption on Functionalized Electrode Surfaces.** Protein adsorption on functionalized surfaces was examined by a Leica DM IL inverted epifluorescence microscope (Leica Microsystems Pty Ltd, USA), fitted with transmitted light LED back illumination and an EL6000 Fluoro system (mercury lamp). The filter sets used in this study are: Cy3 filter cube (BP545/50, a dichroic mirror: 565 and an emission filter: 610/75) for RBITC-Cyt c, and GFP filter cube (BP470/40, a dichroic mirror: 500 and an emission filter: 525/50) for FITC-BSA. Observation and image recording were conducted under two objectives: 10x NA0.22 air and 63× NA1.25 oil. Images were captured using ProgRes Capture Pro 2.7 software by the integrated ProgRes CFscan CCD camera (JENOPTIK Laser, Optik, Systeme GmbH, Germany).

A 1 mg/mL fluorescent dye labeled protein (FITC-BSA or RBITC-Cyt c) solution was prepared in PBS buffer, pH 7.4. The functionalized surfaces were exposed to the fluorescently tagged protein solution at room temperature for 1 h in the dark. After 1 h adsorption, the protein solution was removed, PBS buffer was added into the containers to allow a 5−10 min soaking to remove weakly adsorbed proteins from the surfaces. This step is followed by removal of PBS buffer and replaced with Milli Q water to remove the buffer salts from the protein adsorbed surfaces. Then the protein adsorbed surfaces were dried under a gentle flow of argon gas and mounted face down on to the microscope coverslip (22 × 60 mm No.1, Paul Marienfeld GmbH & Co. KG, Germany).

The gray scale images were taken under the maximum lamp intensity of the fluorescence microscope with the filter set appropriate for the detection of the fluorescent dye. Survey images were taken from each sample under 10× magnification. The optimized exposure time was 6 s for FITC-BSA and 3 s for RBITC-Cyt c. Images recorded under 63x magnification were used for quantitative comparison of protein adsorption on different surfaces. To obtain statistical significance, 3 samples of each type of surface were prepared. From each sample, 10−15 images were captured respectively in the modified and unmodified areas at random locations. The setting of exposure is 3 s for FITC-BSA and 50 ms for RBITC-Cyt c. ImageJ 1.41(National Institutes of Health, USA) was used to process the images. The intensity of the gray scale image, expressed as the gray value, is proportional to the amount of fluorescent labeled protein absorbed on the surface. Therefore, the average gray value (mean gray value) of the images taken under the same instrumental setting (lamp intensity, magnification, and exposure time) was used to compare protein adsorptions between different samples.

**X-ray Photoelectron Spectroscopy Measurement.** XPS spectra were obtained using an EscaLab 220-IXL spectrometer with a monochromated Al Ka source (1486.6 eV), hemispherical analyzer and multichannel detector. The spectra were accumulated at a take-off angle of 90° with a 0.79 $mm^2$ spot size at a pressure of less than $1 \times 10^{-8}$ mbar. Survey scans (0−1100 eV) were carried out with 1.0 eV step size, 100 ms dwell time, and analyzer pass energy 100 eV. High-resolution scans (P2p, S2p, C1s, N1s) were carried out with 0.1 eV step size, 100 ms dwell time, and pass energy 20 eV. Binding energies of elements was corrected with reference to graphite carbon C1s (284.4 eV). The XPS spectrum was analyzed with the curve-fitting program XPSPEAK 4.1 and involved background subtraction using Shirley routine and a subsequent nonlinear least-squares fitting to mixed Gaussian-Lorentzian functions (with Gaussian-Lorentzian ratio of O1s 45%, S2p 30%, C1s 20% , N1s 100%). The atomic ratios of different species on the surfaces were calculated by the normal area of peaks, which is the area under the peaks of the narrow scan spectrum divided by the number of scans and the element sensitivity factor. For the elements considered, the sensitivity factors are S2p 1.68, P2p 1.19, O1s 2.93, C1s 1.00, and N1s 1.80.

## RESULTS AND DISCUSSION

Seven different surfaces were prepared as shown in Figure 1. The two surfaces of interest are the mix-GC and the PPC-GC surfaces. The SP-GC and TMAP-GC surfaces are included to evaluate the anti-biofouling performance of the two surfaces with single charge. The OEG-Ph-GC was incorporated to allow a comparison with our previous studies using surfaces modified with OEG-aryl diazonium salts. The OEG-SAM-Au and C12-SAM-Au surfaces were added to allow comparison with many other studies of anti-biofouling surfaces that employ these surfaces as a good anti-biofouling surface and a good biofouling surface, respectively. The alkanethiol comparison surfaces have been characterized extensively in the literature and the phenyl OEG (hydroxyl terminated) diazonium salt have been reported elsewhere[35,37,38] with further details provided in the Supporting Information (Figure SI 1 and Figure SI 3). The SP-GC, TMAP-GC and mix-GC surface were recently characterized by us in a detailed study showing this mixture forms a surfaces with a 1:1 ratio of TMAP:SP and hence is a zwitterionic surface.[57] Hence, only PPC has never previously been deposited onto an electrode and therefore its characterization will be discussed in detail here.

**X-ray Photoelectron Spectroscopy Characterization of PPC-GC Surfaces.** XPS C1s, N1s, P2p, and O1s core level spectra of glassy carbon surfaces modified with in situ generated phosphorylcholine (PPC) diazonium salt are shown in Figure 2. The nitrogen peak at 402.93 eV (N2) and phosphorous peak

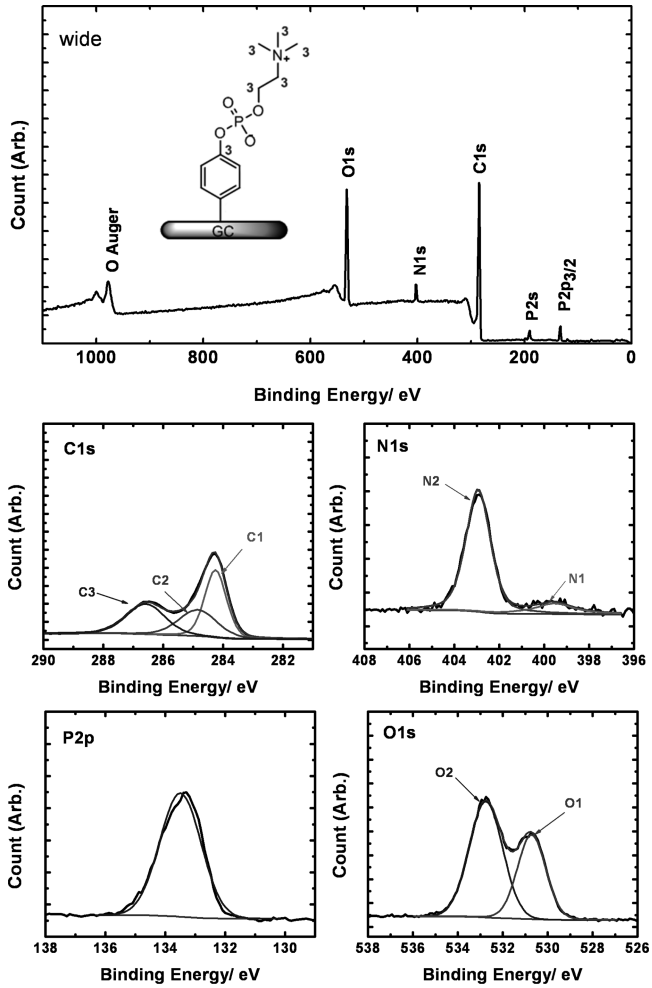


**Figure 2.** X-ray photoelectron spectrum of phenyl phosphorylcholine (PPC) layers on glassy carbon surface. The survey spectrum (with the molecular structure), C1s, N1s, P2p, and O1s core-level spectra.

at 133.49 eV are indicative of the presence of phosphorylcholine.[58] The nitrogen peak at 399.38 eV (N1), is often attributed to an azo linkage in the literature.[59,60] Azo-linkages have been suggested to be a result of the formation of multilayers during the deposition of aryl diazonium salts. However this nitrogen peak is also present on bare glassy carbon surface (see the Supporting Information, Figure SI 2, for details). Nitrogen peaks around 400 eV on clean GC surface have been reported in literature and are presumably due to the organic precursors from which the GC is prepared.[61] The narrow scan of carbon C1s, can be fitted with 3 peaks centered at 284.45 eV (C1), 285.55 eV (C2), and 286.85 eV (C3), which were also observed from bare glassy carbon. Compared with C1s spectrum of bare glassy carbon, there is a significant increase (from ∼5 to ∼20%, see the Supporting Information, Table SI 1) in carbon signal at the binding energy of the C3 peak, which strongly suggests that C3 peak in Figure 2 C1s region mostly arises from PPC-layers. The binding energy correlates to carbon atoms bound to a positively charged nitrogen and to the oxygen in the phoshorylcholine head group (see PPC molecular structure in Figure 2) .[58,62] The C2 peak, which is also observed with a distinct peak on bare glassy is mostly attributed to the adventitious carbon species (C−O and C−N) adsorbed on the carbon substrate.[63] The C1 peak comes from the glassy carbon substrate as well as the aromatic carbon from PPC layers.[64,65]

In the O1s narrow scan, the spectrum can be well-fitted with two peaks centered at 532.75 eV (O2) and 530.73 eV (O1). The source of O2 peak is attributed to be adventitious carbon oxygen species as well as residual water on the surface. The O1 peak is therefore assigned to the oxygen from the phosphorylcholine group as it is not present in the spectrum of the bare surface. The atomic percentage information is provided in the Supporting Information, the calculated P/N2 ratio is approximately 1:1, which correlates well with the molecular structure of phosphorylcholine group.

As previous comparative studies by Gooding and co-workers of the 4-sulfophenyl diazonium salt reductive adsorption on gold and glassy carbon has suggested,[65] it is important to examine the electrochemical stability of the grafted phenyl derivatives in the electrode coatings. Following the same procedure in the studies of SP/TMAP mixed layers by Gui et al.,[57] the PPC-GC and OEG-Ph-GC surfaces were interrogated with repeated cyclic voltammetry scans between −1.0 and 0.8 V in 0.1 M KCl aqueous solution. It was then confirmed by XPS that the chemistry of the two coatings has not changed even after 60 cycles of scans (see Figures SI 3 and SI 4 in the Supporting Information for details).

**Fluorescence Microscopy Evaluation of Nonspecific Adsorption of Protein.** Two proteins were employed to evaluate the ability of different surfaces to limit biofouling; bovine serum albumin (BSA) and cytochrome *c* (Cyt c). The choice of these proteins are primarily because they are anionic and cationic at physiological pH as the isoelectric point (pI) of BSA and Cyt c are 4.8 and 10.0, respectively.[32] We have shown previously that the charge of proteins can have a big influence on their nonspecific adsorption to surfaces.[62] The evaluation of protein adsorption was conducted using fluorescent microscopy with FITC-BSA and RBITC-Cyt c. Representative images of proteins adsorbed at PPC-GC surfaces around the border of the two regions are given in Figure 3. As can be identified in both images, the fluorescence intensity is much higher in the uncoated regions. These intensity differences indicate both BSA and Cyt c were repelled from the PPC modified surface.

Figure 4 shows example 63× images used in quantitative comparison from all seven coatings after exposure to FITC-BSA and the RBITC-Cyt c (for images of bare GC and gold surface, see Figure SI 9 in the Supporting Information). In both rows, it is easy to identify TMAP-GC and C12-SAM-Au as the two most biofouling surfaces towards the adsorption of both BSA and Cyt c. Three surfaces PPC-GC, mix-GC and OEG-SAM-Au are all quite resistant to both proteins as indicated by the much dimmer images. Clear features of aggregation of the adsorbed BSA and Cyt c are observed on the images of OEG-Ph-GC.

The quantitative evaluation of the data has shown the average intensity from the different samples of the same surface chemistry is quite consistent (fluorescence intensity comparison charts between individual samples are provided in the Supporting Information, Figures SI 10−13).

For a systematic comparison, fluorescence intensities of different surfaces are normalized relative to the intensities of C12-SAM-Au surfaces to represent the protein adsorption level. Average intensity of the background has been subtracted prior to normalization. The bar charts in Figure 5 a and b present the quantitative comparison of BSA adsorption and Cyt c adsorption on different electrode surfaces. There are two things one needs to be clear with the charts: (1) the values provided in the diagram do not represent the absolute amount

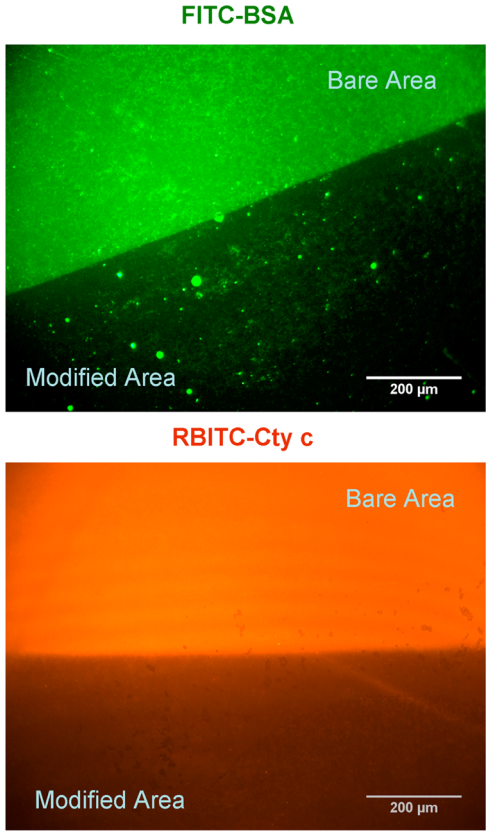


**Figure 3.** Fluorescence microscopic images of FITC-BSA and RBITC-Cyt *c* adsorbed on PPC-GC surfaces under 10× magnification in the area between bare part (unmodified) and the modified part of the glassy carbon surface.

of protein adsorbed on the surface. Hence, whether a surface is more resistant to one protein than the other is not determined by comparing the two charts. (2) Although the absolute quantity of protein adsorbed is unknown, we can compare how effective a surface is at resisting the protein adsorption relative to OEG-SAM-Au and C12-SAM-Au, as the two systems are the known anti-biofouling and biofouling standards in many protein adsorption studies in literature.[32,66,67]

By comparing the adsorption of BSA on various surfaces in Figure 5a, it is readily identified that the surface with the highest adsorption of protein is TMAP-GC, the intensity of which is even higher than C12-SAM-Au (114.4 % ($s$ = 9.3, $n$ = 3) of C12-SAM-Au). OEG-SAM-Au has 14.2 % ($s$ = 2.8, $n$ = 3) of the adsorption on C12-SAM-Au. However, three surfaces (SP-GC, PPC-GC, and mix-GC) having adsorption less than 6 % of the adsorption on C12-SAM-Au. SP-GC has the lowest adsorption of all (almost 0 %), whereas the other two are respectively 3.9% ($s$ = 4.2, $n$ = 3) and 5.4% ($s$ = 6.3, $n$ = 3) of the level of adsorption on C12-SAM-Au. The adsorption on OEG-Ph-GC is 19.3 % ($s$ = 7.9, $n$ = 3) of the adsorption on C12-SAM-Au, slightly higher than OEG-SAM-Au. The comparison of Cyt c adsorption in Figure 5b shows that the OEG-SAM-Au, PPC-GC, and mix-GC present similar levels of adsorption and are the three lowest ones (~24% of the adsorption on C12-SAM-Au).

To summarize, the two zwitterionic surfaces, PPC-GC and mix-GC, are as effective as OEG-SAM-Au at resisting Cyt c adsorption and more effective than OEG-SAM-Au at resisting the adsorption of BSA. The performance of PPC-GC is slightly


dx.doi.org/10.1021/am400519m | ACS Appl. Mater. Interfaces 2013, 5, 4827−4835

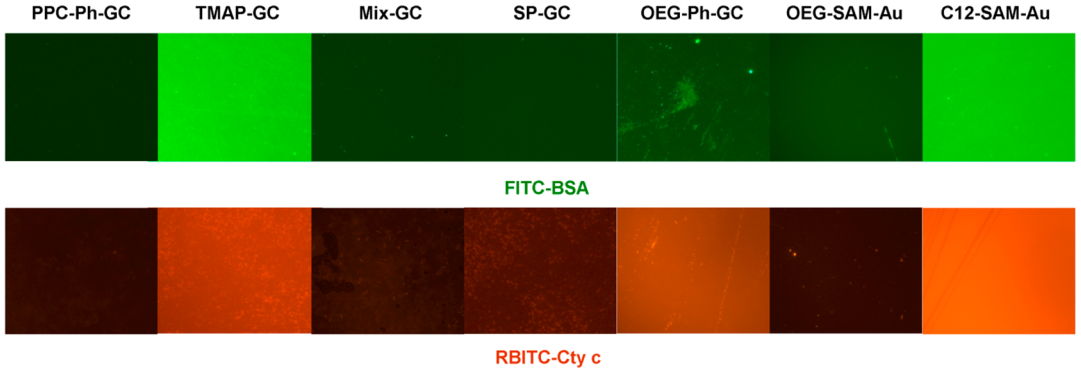


**Figure 4.** Fluorescence microscopic images recorded under 63x magnification from FITC-BSA (top image row) and RBITC-Cyt *c* (bottom image row) adsorbed all seven different surfaces.

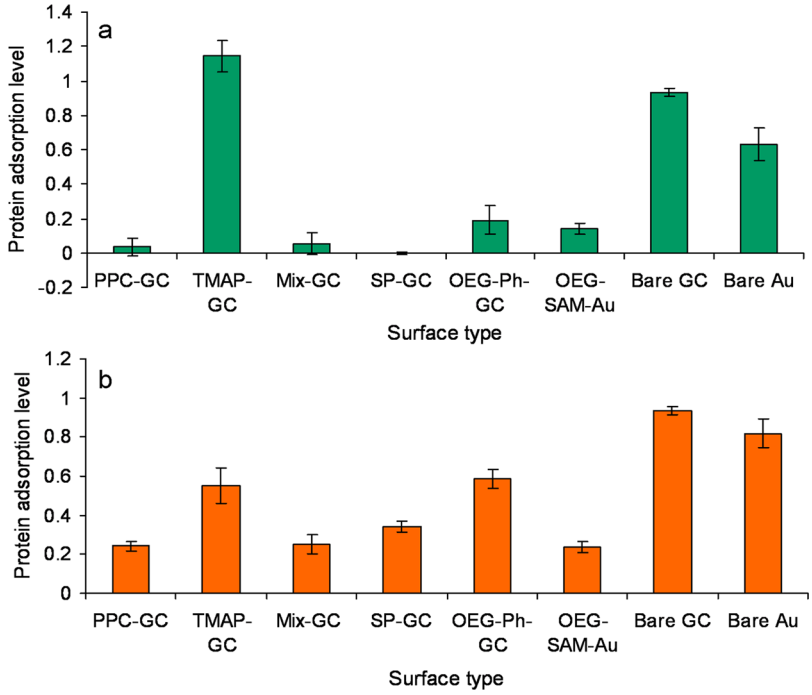


**Figure 5.** FITC-BSA adsorption level (a) and RBITC-Cyt *c* adsorption level (b) at different surfaces represented by the normalized fluorescence intensities (relative to C12-SAM-Au). The error bar represents the standard deviation between each of 3 samples of the same surface chemistry.

**Table 1. Charge Transfer Resistance and Electron Transfer Rate Comparison of Different Surfaces to $Fe(CN)_6^{3-}$ and $Ru(NH_3)_6^{3+}$ in Aqueous Solution[a]**

| | ferricyanide ($Fe(CN)_6^{3-}$) | | hexaammineruthenium ($Ru(NH_3)_6^{3+}$) | |
|---|---|---|---|---|
| | $R_{ct}$ ($\Omega$ cm$^2$) | $k_{et} \times 10^{-3}$ (cm s$^{-1}$) | $R_{ct}$ ($\Omega$ cm$^2$) | $k_{et} \times 10^{-3}$ (cm s$^{-1}$) |
| PPC -GC | 559.7 ($s$ = 31.1) | 0.48 ($s$ = 0.03) | 36.7 ($s$ = 5.7) | 7.4 ($s$ = 1.2) |
| mix-GC | 254.4 ($s$ = 54.5) | 1.09 ($s$ = 0.26) | 34.3 ($s$ = 2.1) | 7.8 ($s$ = 0.5) |
| OEG-Ph-GC | 1898.1 ($s$ = 263.4) | 0.14 ($s$ = 0.02) | 223.4 ($s$ = 32.5) | 1.21 ($s$ = 0.16) |
| OEG-SAM-Au | 10256.7 ($s$ = 963.7) | 0.034 ($s$ = 0.009) | 6766.1 ($s$ = 191.3) | 0.041 ($s$ = 0.013) |
| C12-SAM-Au | 44785.4 ($s$ = 1653.6) | 0.0065 ($s$ = 0.0024) | 25863.3 ($s$ = 693.5) | 0.011 ($s$ = 0.004) |
| bare GC | 15.4 ($s$ = 0.2) | 17.6 ($s$ = 0.3) | 1.29 ($s$ = 0.02) | 210.2 ($s$ = 2.9) |
| bare Au | 9.4 ($s$ = 0.8) | 28.9 ($s$ = 2.8) | 0.71 ($s$ = 0.08) | 380.9 ($s$ = 47.9) |

[a]Average values and standard deviation ($s$) were calculated from the measurement of 3 ($n$ = 3) electrodes in each experiment.

better than mix-GC. The anti-biofouling ability of OEG-Ph-GC is significantly inferior to OEG-SAM-Au. The observation of moderate protein resistance of OEG-Ph-GC is generally consistent with previous studies on methoxy terminated phenyl oligo(ethylene glycol) layers on GC surfaces.[52,68] The adsorption behavior of proteins at TMAP-GC and SP-GC seems to be affected by the charge interaction between protein and the surface, except that SP-GC is repelling Cyt *c* despite them being oppositely charged to each other. The apparent inconsistency regarding charge repulsion on the protein

Table 2. Charge Transfer Resistance of Different Surfaces Measured in $Fe(CN)_6^{3-}$ Solution and $Ru(NH_3)_6^{3+}$ Solution before and after 1 h Exposure to BSA[a]

| | $R_{ct}$ ($\Omega$ cm$^2$) (in $Fe(CN)_6^{3-}$ solution) | | $R_{ct}$ ($\Omega$ cm$^2$) (in $Ru(NH_3)_6^{3+}$ solution) | |
|---|---|---|---|---|
| | before 1 h BSA adsorption | after 1 h BSA adsorption | before 1 h BSA adsorption | after 1 h BSA adsorption |
| PPC-GC | 809.3 ($s$ = 15.7) | 807.9 ($s$ = 16.7) | 42.3 ($s$ = 1.1) | 44.3 ($s$ = 1.1) |
| mix-GC | 185.6 ($s$ = 2.0) | 178.3 ($s$ = 1.9) | 26.02 ($s$ = 1.24) | 25.2 ($s$ = 1.3) |
| OEG-Ph-GC | 1899.3 ($s$ = 165.1) | 3734.1 ($s$ = 233.3) | 192.6 ($s$ = 3.1) | 556.4 ($s$ = 9.6) |
| OEG-SAM-Au | 10342.2 ($s$ = 130.9) | 10226.5 ($s$ = 131.1) | 6299.4 ($s$ = 296.7) | 6222.3 ($s$ = 315.7) |
| C12-SAM-Au | 30874.6 ($s$ = 1423.4) | 49461.7 ($s$ = 1821.4) | 14373.2 ($s$ = 157.6) | 18947.9 ($s$ = 183.4) |
| bare GC | 15.3 ($s$ = 0.7) | 92.3 ($s$ = 1.1) | 1.3 ($s$ = 0.9) | 19.2 ($s$ = 1.3) |
| bare Au | 10.3 ($s$ = 0.6) | 29.2 ($s$ = 0.6) | 0.8 ($s$ = 0.2) | 11.5 ($s$ = 1.5) |

[a]Average values and standard deviation ($s$) were calculated from the measurement of 3 ($n$ = 3) electrodes in each experiment.

adsorption at SP-GC surface, can be attributed to the hypothesis of kosmotrope-based protein resistance raised by Kane et al.[69] According to the hypothesis, surfaced presenting kosmotropes or molecules that have a structure similar to he known kosmotropes are protein-resistant. The sulfonic group exposed on SP coating of the electrode surface is similar in structure to the known kosmotropic anion $SO_4^{2-}$.[70,71] Hence, the resistance of SP-GC to positively charged proteins might be attributed to the kosmotropic effect.

**Electrochemical Impedance Spectroscopy of the Different Surfaces.** The two zwitterionic surfaces PPC-GC and mix-GC exhibit much better performance at resisting protein adsorption compared with OEG-Ph-GC. But are they low impedance layers? To evaluate the passivating ability of the difference modification layers, we performed the electrochemistry of the redox probes, $Fe(CN)_6^{3-}$ and $Ru(NH_3)_6^{3+}$, using CVs (see the Supporting Information, Figures SI 6 and SI 7) and electrochemical impedance spectroscopy (EIS) in physiological buffer. As displayed in Table 1, the charge transfer resistance $R_{ct}$ and calculated rate constants $k_{et}$ of $Fe(CN)_6^{3-}$ and $Ru(NH_3)_6^{3+}$ on the bare electrode surfaces compare favorably with the literature.[72−76] Apart from the two bare surfaces presenting the lowest $R_{ct}$, the comparison of charge transfer resistance between coated surfaces has shown essentially the same trend for both $Fe(CN)_6^{3-}$ and $Ru(NH_3)_6^{3+}$ solutions. The mix-GC surface exhibited the lowest $R_{ct}$ of all modified surfaces, followed by PPC-GC, and then OEG-Ph-GC. OEG-SAM-Au and C12-SAM-GC are 2 orders of magnitude higher in $R_{ct}$ than phenyl layers based surfaces. The high $R_{ct}$ of OEG-SAM-Au and C12-SAM-Au surfaces is expected because these molecules form closely packed SAMs because of the long-chain alkanethiols.

The low impedance of the mix-GC and PPC-GC surfaces is also shown in the CVs (see the Supporting Information, Figures SI 6 and SI 7) where despite the presence of an organic layer on the electrode there is still significant Faradaic signal to the redox species in solution; thus indicating the electrode is not completely passivated by the organic layer. The low $R_{ct}$ of the two zwitterionic surfaces PPC-GC and mix-GC implies the surface coatings are thin and/or loosely packed. The $R_{ct}$ of OEG-Ph-GC is one order of magnitude higher than the two zwitterionic surfaces, however, considerably lower than the alkanethiol based SAMs, which suggests the OEG phenyl derivative form layers that are poorly packed, such that the underlying glassy carbon surface may be open and accessible to species in solution, which is consistent with the inferior anti-biofouling properties of this surface.[52]

Next, EIS was also used to evaluate the nonspecific adsorption of BSA as this is a more realistic test of how these surfaces will actually be used than the microscopy imaging. The BSA adsorbed electrodes were conducted following the same procedure for preparation of the samples for fluorescence microscope, except unlabeled protein was used. After initial measurements, a control experiment was performed before the BSA adsorption, which is to expose all the electrodes to PBS, pH 7.4 for 1 h. This control experiment is to examine any changes to the coatings caused by buffer salts adsorption or absorbing of water. CVs and Nyquist plots are provided in the Supporting Information (Figures SI 14−16).

Table 2 presents the results of the $R_{ct}$ measurement of various surfaces before and after BSA adsorption. No significant changes were observed for any surface between before and after 1 h incubation in PBS alone. To both $Fe(CN)_6^{3-}$ and $Ru(NH_3)_6^{3+}$, only 4 surfaces showed a significant increase in $R_{ct}$ when exposed to BSA solutions. These were OEG-Ph-GC, C12-SAM-Au, and the two bare surfaces. The exposure to BSA solution caused no significant change to PPC-GC, mix-GC, and OEG-SAM-Au surfaces in terms of the value of $R_{ct}$. This observation indicates the resistance of the three surfaces to the adsorption of BSA, which agrees well with the result of fluorescence microscope experiment. For OEG-Ph- GC, C12-SAM-Au, bare GC and bare Au, the increase of $R_{ct}$ is due to the substantial amount of BSA adsorption forming insulating layers that hinder the electron transfer.[77]

## CONCLUSION

The fluorescence microscopy and EIS results together show we have achieved our objective of forming anti-biofouling coatings for electrodes that do not completely passivate the electrode from undergoing Faradaic electrochemistry after being modified with the organic layer. This was achieved using either an aryl diazonium salt bearing a zwitterionic group, namely, phenyl phosphorylcholine (PPC) diazonium salt, or a mixture of sulfophenyl aryl diazonium salt and trimethylammonium phenyl aryl diazonium salt (mix-GC) that form a 1:1 ratio on the electrode surface. Both the PPC and mix-GC surfaces are zwitterionic and form thin layers on the electrodes. The performance of these surfaces were compared to oligo(ethylene oxide) modified surfaces as classical anti-biofouling surfaces and surfaces that are known to be fouled by proteins. The aryl diazonium salt derived layers were found to be highly electrochemically stable on electrode surfaces and provide superior resistance to protein fouling to both cationic and anionic proteins than 2-(2-(2-phenoxy)ethoxy)-ethoxy)-ethanol (OEG-Ph) on glassy carbon surfaces. In fact the PPC-GC and mix-GC layers are as effective as the "gold standard" of oligo(ethylene oxide) alkanethiol self-assembled monolayers on gold electrodes (OEG-SAM-Au) at resisting nonspecific

adsorption of positively charged protein Cyt c and performed even better than OEG-SAM-Au at resisting the adsorption of negatively charged protein BSA.

EIS studies have revealed that zwitterionic surfaces PPC-GC and mix-GC exhibit greatly lower impedance to soluble redox probes than OEG SAMs. PPC coating and mix coating both presented orders of magnitude lower impedance than OEG-Ph coating. The EIS study of BSA adsorption on different surfaces has suggested PPC and mix coatings are effective at preventing protein fouling to the electrode surfaces. The current studies have shown the promising future of using zwitterionic phenyl layers as low impedance anti-biofouling coating to the electrode surface with greater long-term stability, for improving in vitro and in vivo performance of electrochemical biosensors and implantable electrodes. Future work will be directed towards extending these modifying layers on electrodes to studies of cell adhesion to electrode surfaces as well as demonstrating biologically important redox species can also be detected.

## ■ ASSOCIATED CONTENT

### Ⓢ Supporting Information

Electrochemical reduction of PPC and OEG-Ph;XPS analysis of OEG-Ph-GC; electrochemical stability of PPC-GC and OEG-Ph-GC; cyclic voltammetry and impedance spectroscopy of PPC-GC, mix-GC, OEG-Ph-GC, OEG-SAM-Au, and C12-SAM-Au surfaces; and additional fluorescence microscope image and electrochemistry data for protein adsorption on electrode surfaces. This material is available free of charge via the Internet at http://pubs.acs.org.

## ■ AUTHOR INFORMATION

### Corresponding Author

*E-mail: justin.gooding@unsw.edu.au.

### Present Addresses

[†]Alicia L. Gui is currently at Institut für Reine und Angewandte, Carl von Ossietzky Universität Oldenburg, Oldenburg, 26111, Germany.

[‡]Erwann Luais is currently at GREMAN, Université François Rabelais, Tours, 37200, France.

### Author Contributions

The manuscript was written through contributions of all authors. All authors have given approval to the final version of the manuscript.

### Notes

The authors declare no competing financial interest.

## ■ ACKNOWLEDGMENTS

The authors thank the Australian Research Council (LP100200593), and the Australian Government for funding and the University of New South Wales for the scholarship for A.L.G.

## ■ REFERENCES

(1) Castner, D. G.; Ratner, B. D. *Surf. Sci* **2002**, *500*, 28−60.
(2) Gifford, R.; Kehoe, J. J.; Barnes, S. L.; Kornilayev, B. A.; Alterman, M. A.; Wilson, G. S. *Biomaterials* **2006**, *27*, 2587−2598.
(3) Vaddiraju, S.; Tomazos, I.; Burgess, D. J.; Jain, F. C.; Papadimitrakopoulos, F. *Biosens. Bioelectron.* **2010**, *25*, 1553−1565.
(4) Gooding, J. J. *Electroanal* **2008**, *20*, 573−582.
(5) Ronkainen, N. J.; Halsall, H. B.; Heineman, W. R. *Chem. Soc. Rev.* **2010**, *39*, 1747−1763.
(6) Sankaranarayanan, S.; Singh, R.; Bhethanabotla, V. R. *J. Appl. Phys.* **2010**, 108.
(7) Trouillon, R.; O'Hare, D. *Electrochim. Acta* **2010**, *55*, 6586−6595.
(8) Cogan, S. F. *Annu. Rev. Biomed. Eng.* **2008**, *10*, 275−309.
(9) Merrill, D. R.; Bikson, M.; Jefferys, J. G. R. *J. Neurosci. Meth.* **2005**, *141*, 171−198.
(10) Banerjee, I.; Pangule, R. C.; Kane, R. S. *Adv. Mater.* **2011**, *23*, 690−718.
(11) Llanos, G. R.; Sefton, M. V. *J. Biomed. Mater. Res* **1993**, *27*, 1383−1391.
(12) McPherson, T.; Kidane, A.; Szleifer, I.; Park, K. *Langmuir* **1998**, *14*, 176−186.
(13) Jenney, C. R.; Anderson, J. M. *J. Biomed. Mater. Res* **1999**, *44*, 206−216.
(14) Leckband, D.; Sheth, S.; Halperin, A. *J. Biomater. Sci., Polym. Ed.* **1999**, *10*, 1125−1147.
(15) Deible, C. R.; Petrosko, P.; Johnson, P. C.; Beckman, E. J.; Russell, A. J.; Wagner, W. R. *Biomaterials* **1999**, *20*, 101−109.
(16) Bearinger, J. P.; Terrettaz, S.; Michel, R.; Tirelli, N.; Vogel, H.; Textor, M.; Hubbell, J. A. *Nature. Mater* **2003**, *2*, 259−264.
(17) Prime, K. L.; Whitesides, G. M. *Science* **1991**, *252*, 1164−1167.
(18) Harder, P.; Grunze, M.; Waite, J. H. *J. Adhes.* **2000**, *73*, 161−177.
(19) Boozer, C.; Yu, Q. M.; Chen, S. F.; Lee, C. Y.; Homola, J.; Yee, S. S.; Jiang, S. Y. *Sens. Actuators, B* **2003**, *90*, 22−30.
(20) Choi, S.; Murphy, W. L. *Langmuir* **2008**, *24*, 6873−6880.
(21) Hodneland, C. D.; Mrksich, M. *J. Am. Chem. Soc.* **2000**, *122*, 4235−4236.
(22) Roberts, C.; Chen, C. S.; Mrksich, M.; Martichonok, V.; Ingber, D. E.; Whitesides, G. M. *J. Am. Chem. Soc.* **1998**, *120*, 6548−6555.
(23) Umek, R. M.; Lin, S. W.; Vielmetter, J.; Terbrueggen, R. H.; Irvine, B.; Yu, C. J.; Kayyem, J. F.; Yowanto, H.; Blackburn, G. F.; Farkas, D. H.; Chen, Y. P. *J. Mol. Diagn.* **2001**, *3*, 74−84.
(24) Liu, G. Z.; Gooding, J. J. *Langmuir* **2006**, *22*, 7421−7430.
(25) Liu, G.; Iyengar, S. G.; Gooding, J. J. *Electroanalysis* **2012**, *24*, 1509−1516.
(26) Lloyd, A. W.; Dropcova, S.; Faragher, R. G. A.; Gard, P. R.; Hanlon, G. W.; Mikhalovsky, S. V.; Olliff, C. J.; Denyer, S. P.; Letko, E.; Filipec, M. *J. Mater. Sci.−Mater. Med.* **1999**, *10*, 621−627.
(27) Luk, Y. Y.; Kato, M.; Mrksich, M. *Langmuir* **2000**, *16*, 9604−9608.
(28) Talarico, T.; Swank, A.; Privalle, C. *Biochem. Biophys. Res. Commun.* **1998**, *250*, 354−358.
(29) Hayward, J. A.; Chapman, D. *Biomaterials* **1984**, *5*, 135−142.
(30) Lewis, A. L.; Driver, M. *J. Chem. Educ.* **2002**, *79*, 321−326.
(31) Yamasaki, A.; Imamura, Y.; Kurita, K.; Iwasaki, Y.; Nakabayashi, N.; Ishihara, K. *Colloids Surf., B* **2003**, *28*, 53−62.
(32) Holmlin, R. E.; Chen, X. X.; Chapman, R. G.; Takayama, S.; Whitesides, G. M. *Langmuir* **2001**, *17*, 2841−2850.
(33) Tegoulia, V. A.; Rao, W. S.; Kalambur, A. T.; Rabolt, J. R.; Cooper, S. L. *Langmuir* **2001**, *17*, 4396−4404.
(34) Chen, S. F.; Yu, F. C.; Yu, Q. M.; He, Y.; Jiang, S. Y. *Langmuir* **2006**, *22*, 8186−8191.
(35) Chen, S. F.; Zheng, J.; Li, L. Y.; Jiang, S. Y. *J. Am. Chem. Soc.* **2005**, *127*, 14473−14478.
(36) Chung, Y. C.; Chiu, Y. H.; Wu, Y. W.; Tao, Y. T. *Biomaterials* **2005**, *26*, 2313−2324.
(37) Kitano, H.; Kawasaki, A.; Kawasaki, H.; Morokoshi, S. *J. Colloid Interface Sci.* **2005**, *282*, 340−348.
(38) Chen, S. F.; Jiang, S. Y. *Adv. Mater.* **2008**, *20*, 335−338.
(39) Shi, Q.; Su, Y. L.; Zhao, W.; Li, C.; Hu, Y. H.; Jiang, Z. Y.; Zhu, S. P. *J. Membrane. Sci.* **2008**, *319*, 271−278.
(40) Pinson, J.; Podvorica, F. *Chem. Soc. Rev.* **2005**, *34*, 429−439.
(41) Belanger, D.; Pinson, J. *Chem. Soc. Rev.* **2011**, *40*, 3995−4048.
(42) Gooding, J. J.; Liu, G. Z.; Gui, A. L. The Use of Aryl Diazonium Salts in the Fabrication of Biosensors and Chemical Sensors. In *Aryl Diazonium Salts: New Coupling Agents in Polymer and Surface Science* , 1 June 2012 ed.; Chehimi, M. M., Ed.; Wiley−VCH Verlag GmbH & Co. KGaA: Weinheim, Germany, 2012; pp 197−218.
(43) Mahouche-Chergui, S.; Gam-Derouich, S.; Mangeney, C.; Chehimi, M. M. *Chem. Soc. Rev.* **2011**, *40*, 4143−4166.

(44) Fond, A. M.; Birenbaum, N. S.; Felton, E. J.; Reich, D. H.; Meyer, G. J. *J. Photochem. Photobiol., A* **2007**, *186*, 57−64.
(45) Reichert, U.; Linden, T.; Belfort, G.; Kula, M. R.; Thommes, J. *J. Membr. Sci.* **2002**, *199*, 161−166.
(46) Tessler, L. A.; Reifenberger, J. G.; Mitra, R. D. *Anal. Chem.* **2009**, *81*, 7141−7148.
(47) Clare, T. L.; Clare, B. H.; Nichols, B. M.; Abbott, N. L.; Hamers, R. J. *Langmuir* **2005**, *21*, 6344−6355.
(48) Heyes, C. D.; Kobitski, A. Y.; Amirgoulova, E. V.; Nienhaus, G. U. *J. Phys. Chem. B* **2004**, *108*, 13387−13394.
(49) Zernla, J.; Lekka, M.; Wiltowska-Zuber, J.; Budkowski, A.; Rysz, J.; Raczkowska, J. *Langmuir* **2008**, *24*, 10253−10258.
(50) Damodaran, V. B.; Fee, C. J.; Popat, K. C. *Appl. Surf. Sci.* **2010**, *256*, 4894−4901.
(51) Dintelmann, T. S.; Heimann, K.; Kayatz, P.; Schraermeyer, U. *Graefes Arch. Clin. Exp. Ophthalmol.* **1999**, *237*, 830−839.
(52) Downard, A. J.; Jackson, S. L.; Tan, E. S. Q. *Aust. J. Chem.* **2005**, *58*, 275−279.
(53) Roque, A. C. A.; Bispo, S.; Pinheiro, A. R. N.; Antunes, J. M. A.; Goncalves, D.; Ferreira, H. A. *J. Mol. Recognit.* **2009**, *22*, 77−82.
(54) Togashi, D. M.; Ryder, A. G.; Heiss, G. *Colloids Surf., B* **2009**, *72*, 219−229.
(55) Veiseh, M.; Zhang, M. Q. *J. Am. Chem. Soc.* **2006**, *128*, 1197−1203.
(56) Baranton, S.; Belanger, D. *J. Phys. Chem. B* **2005**, *109*, 24401−24410.
(57) Gui, A. L.; Yau, H. M.; Thomas, D. S.; Chockalingam, M.; Harper, J. B.; Gooding, J. J. *Langmuir* **2013**, *29*, 4772−81.
(58) Fabianowski, W.; Coyle, L. C.; Weber, B. A.; Granata, R. D.; Castner, D. G.; Sadownik, A.; Regen, S. L. *Langmuir* **1989**, *5*, 35−41.
(59) Yu, S. S. C.; Tan, E. S. Q.; Jane, R. T.; Downard, A. J. *Langmuir* **2007**, *23*, 11074−11082.
(60) Shewchuk, D. M.; McDermott, M. T. *Langmuir* **2009**, *25*, 4556−4563.
(61) Allongue, P.; Delamar, M.; Desbat, B.; Fagebaume, O.; Hitmi, R.; Pinson, J.; Saveant, J. M. *J. Am. Chem. Soc.* **1997**, *119*, 201−207.
(62) Ng, C. C. A.; Ciampi, S.; Harper, J. B.; Gooding, J. J. *Surf. Sci.* **2010**, *604*, 1388−1394.
(63) Liu, G. Z.; Liu, J. Q.; Bocking, T.; Eggers, P. K.; Gooding, J. J. *Chem. Phys.* **2005**, *319*, 136−146.
(64) Ciampi, S.; Bocking, T.; Kilian, K. A.; James, M.; Harper, J. B.; Gooding, J. J. *Langmuir* **2007**, *23*, 9320−9329.
(65) Gui, A. L.; Liu, G. Z.; Chockalingam, M.; Le Saux, G.; Harper, J. B.; Gooding, J. J. *Electroanalysis* **2010**, *22*, 1283−1289.
(66) Chapman, R. G.; Ostuni, E.; Takayama, S.; Holmlin, R. E.; Yan, L.; Whitesides, G. M. *J. Am. Chem. Soc.* **2000**, *122*, 8303−8304.
(67) Ostuni, E.; Chapman, R. G.; Holmlin, R. E.; Takayama, S.; Whitesides, G. M. *Langmuir* **2001**, *17*, 5605−5620.
(68) Fairman, C. The preparation and modification of thin carbon films. *PhD Thesis*, The University of New South Wales, Sydney, Australia, 2011.
(69) Kane, R. S.; Deschatelets, P.; Whitesides, G. M. *Langmuir* **2003**, *19*, 2388−2391.
(70) Lawal, O. S. *Food Chem.* **2006**, *95*, 101−107.
(71) Chaplin, M. Kosmotropes and Chaotropes; http://www.lsbu.ac.uk/water/kosmos.html (accessed 26.07.2011).
(72) Blackstock, J. J.; Rostami, A. A.; Nowak, A. M.; McCreery, R. L.; Freeman, M. R.; McDermott, M. T. *Anal. Chem.* **2004**, *76*, 2544−2552.
(73) Ranganathan, S.; McCreery, R.; Majji, S. M.; Madou, M. *J. Electrochem. Soc.* **2000**, *147*, 277−282.
(74) Velmurugan, J.; Sun, P.; Mirkin, M. V. *J. Phys. Chem. C* **2009**, *113*, 459−464.
(75) Mendez, E.; Worner, M.; Lages, C.; Cerda, M. F. *Langmuir* **2008**, *24*, 5146−5154.
(76) Khoshtariya, D. E.; Dolidze, T. D.; Vertova, A.; Longhi, M.; Rondinini, S. *Electrochem. Commun.* **2003**, *5*, 241−245.
(77) Moulton, S. E.; Barisci, J. N.; Bath, A.; Stella, R.; Wallace, G. G. *Electrochim. Acta* **2004**, *49*, 4223−4230.